2.1.3 Corner Analysis

Corner analysis [17] is a simple method to study impacts of fabrication variations on the performance of SOI devices. For our broadband 3-dB coupler design, we consider a ±10 nm variations for the width and the thickness of coupler waveguide, i.e., Δw and Δh, respectively. Figure 2.6(a) illustrates the 4 process corners in the analysis. For each process point, FDTD simulation is conducted; all simulation results are collected to understand the device's tolerance to fabrication. Figure 2.6(b) shows corner analysis results for the coupling imbalance of the broadband 3-dB coupler design, which indicates a worst-case imbalance of 16.7% within a 100 nm bandwidth.

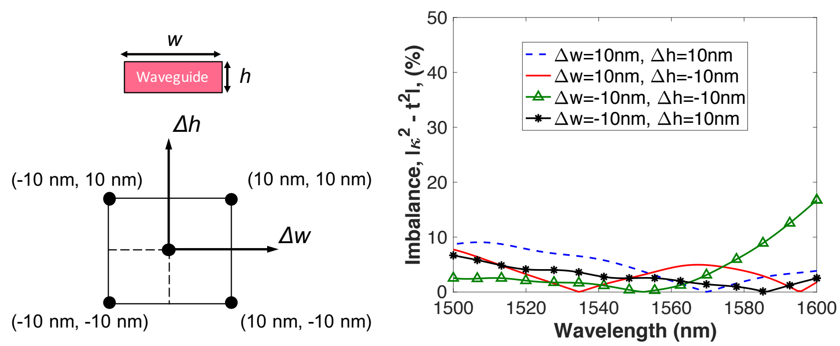

(a) (b)

Figure 2.6: Corner analysis for the broadband 3-dB coupler design. (a) Process corners; (b) corner analysis results for the coupling imbalance, $|\kappa^2 - t^2|$.

2.1.4 Characterization Results

The broadband 3-dB coupler design was fabricated using an electron-beam lithography process at the University of Washington. We used an indirect measurement method to characterize the performance of the fabricated devices. As shown in Fig. 2.7, the indirect measurement structure is an imbalanced MZI circuit, which includes two identical under test couplers for splitting at the input and combining at the output, and two imbalanced

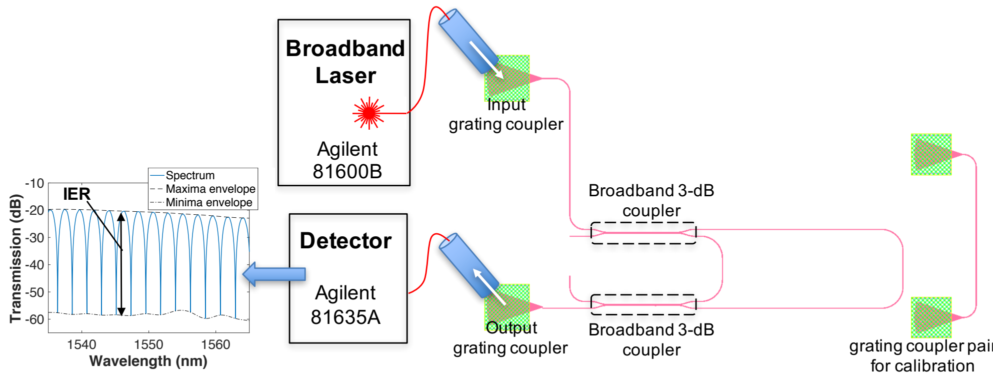

Figure 2.7: Block diagram illustrating the indirect measurement.

phase arms with a length difference, ΔL, of 259.4 μm. Grating couplers (GCs) [53] were used to couple light into and out of the MZI circuit. The measurement structure also includes a pair of GCs connected by a short waveguide, which is intended for calibrating the insertion losses of GCs. In the measurements, an Agilent 81600B tunable laser was used as the optical input source, and an Agilent 81635A optical power sensor was used as the output detector for the MZI circuit.

The κ^2 and t^2 of the under test couplers can be extracted from the interference extinction ratio (IER) of the MZI output spectrum, which is discussed in Appendix C. We define IER as the difference on a logarithmic scale between the minima and maxima transmissions, as illustrated in Fig. 2.7. The wavelength-dependent IERs can be obtained by fitting the envelopes on the minima and maxima of the MZI spectrum. The extracted κ^2 and t^2 are given by:

$$\kappa^2 = \frac{1}{2}\left(1 \pm \frac{1}{\sqrt{10^{IER/10}}}\right) \tag{2.8}$$

$$t^2 = 1 - \kappa^2 \tag{2.9}$$

where we assume that the propagation losses of the two phase arms of the imbalanced MZI circuit are the same and the couplers are lossless. Due to the fact that IERs of the MZI spectrum are independent to the insertion loss of the MZI circuit (e.g., misalignment loss), the κ^2 and t^2 of couplers can be accurately extracted.

Figures 2.8(a) shows the measured spectrum for the MZI circuit, in which the insertion loss introduced by the GCs have been calibrated out. According to the results, the insertion loss of the MZI circuit is less than 1 dB, which indicates the insertion loss of each coupler is less than 0.5 dB. Based on the IERs from the MZI spectrum, we extracted the κ^2 and t^2 of the fabricated couplers using Eqs. 2.8 and 2.9, and the extracted results are shown in Fig. 2.8(b). According to the extracted data, the coupler exhibits a maximum imbalance of 4.7% within a 100 nm wavelength bandwidth from 1500 nm to 1600 nm, which is in good agreement with the FDTD simulation results given in Fig. 2.5(c).

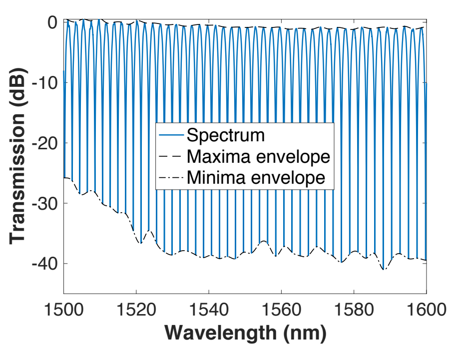

(a)

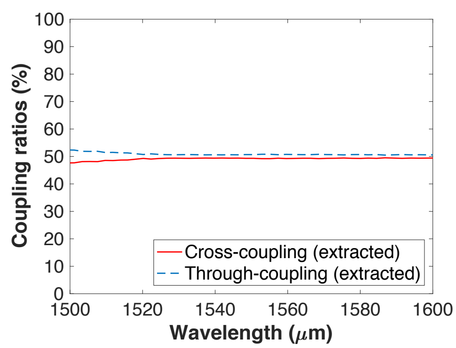

(b)

Figure 2.8: (a) Measured spectrum for the MZI circuit; (b) extracted coupling ratios of the fabricated broadband 3-dB couplers.

2.2 Broadband Mach-Zehnder Interferometer Switch

2.2.1 Design

We have designed a 2×2, TE_0 mode, broadband MZI switch based on the demonstrated TE_0 mode, broadband 3-dB coupler. Figure 2.9(a) shows the schematic for such a switch design, which has a thermo-optic phase shifter on each phase arm and two broadband 3-dB couplers. We modeled the broad-

Appendix B

Derivation of the Transfer Functions of a MZI Switch

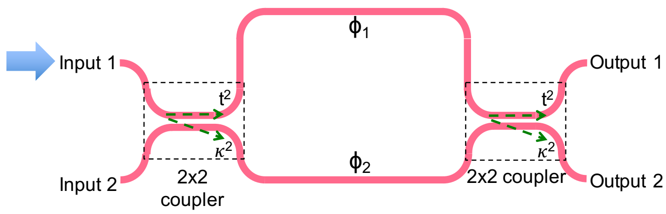

Figure B.1: Schematic for a typical Mach-Zehnder interferometer (MZI) circuit.

Here, we derive the output transfer functions of a MZI switch using the transfer matrix method. Considering a typical MZI circuit as shown in Fig. B.1, the relationship between the input and output electric fields of the MZI circuit can be expressed by:

$$\begin{bmatrix} E_{out1} \\ E_{out2} \end{bmatrix} = \begin{bmatrix} t & -j\kappa \\ -j\kappa & t \end{bmatrix} \begin{bmatrix} e^{-j\phi_1} & 0 \\ 0 & e^{-j\phi_2} \end{bmatrix} \begin{bmatrix} t & -j\kappa \\ -j\kappa & t \end{bmatrix} \begin{bmatrix} E_{in1} \\ E_{in2} \end{bmatrix} \tag{B.1}$$

where E_{in1} and E_{in2} are the electric fields at the two inputs, and E_{out1} and E_{out2} represent the electric fields at the two outputs; t and κ are the through-coupling coefficient and cross-coupling coefficient, respectively, for each 2×2 coupler, and the 2×2 couplers in the MZI are assumed to be identical; ϕ_1 and ϕ_2 are the optical phase shifts of the two phase arms.

Assuming light is launched into the input 1 only, i.e., $E_{in1} = 1$ and

$E_{in2} = 0$, the output electric fields of the circuit are given by:

$$E_{out1} = t^2 e^{-j\phi_1} - \kappa^2 e^{-j\phi_2} \tag{B.2}$$

$$E_{out2} = -j\kappa t e^{-j\phi_1} - j\kappa t e^{-j\phi_2} \tag{B.3}$$

And accordingly, output transmissions are given by:

$$P_{out1} = |E_{out1}|^2 = (\kappa^4 + t^4 - 2\kappa^2 t^2 \cos(\Delta\phi)) \tag{B.4}$$

$$P_{out2} = |E_{out2}|^2 = 2\kappa^2 t^2 (1 + \cos(\Delta\phi)) \tag{B.5}$$

where $\Delta\phi = |\phi_1 - \phi_2|$ is the phase difference between the two waveguide arms. The input light to the MZI circuit can be selectively switched to either of the outputs depending on the phase difference, $\Delta\phi$.

For a $\Delta\phi$ of 0, Eqs. B.4 and B.5 can be simplified as:

$$P_{out1} = (\kappa^2 - t^2)^2 \tag{B.6}$$

$$P_{out2} = 4\kappa^2 t^2 \tag{B.7}$$

Due to the fact that the 2×2 couplers are designed for balanced coupling, i.e., κ^2 and t^2 are equal or close to 0.5, we have $P_{out2} > P_{out1}$, i.e., the switch operates in the cross switching state and routes the input light to the output 2. In such a state, we define the switching ER as:

$$ER_{cross} = 10\log_{10}(\frac{P_{out2}}{P_{out1}}) = 10\log_{10}(\frac{4\kappa^2 t^2}{(\kappa^2 - t^2)^2}) \tag{B.8}$$

As it is shown that the cross state ER is dependent to the coupling ratios, κ^2 and t^2, of the 2×2 couplers in the MZI circuit.

For a $\Delta\phi$ of π, Eqs. B.4 and B.5 can be simplified as:

$$P_{out1} = (\kappa^2 + t^2)^2 \tag{B.9}$$

$$P_{out2} = 0 \tag{B.10}$$

In this case, the switch operates in the bar state, which routes the input light to the output 1. We define the switching ER at the bar state as:

$$ER_{bar} = 10\log_{10}(\frac{P_{out1}}{P_{out2}}) = 10\log_{10}(\frac{(\kappa^2+t^2)^2}{0}) = \infty \tag{B.11}$$

As we can see that the bar state ER is infinite and is independent to the coupling ratios, κ^2 and t^2, of the 2×2 couplers in the MZI circuit. Note that the bar state results given in Eqs. B.9, B.10, and B.11 are based on the assumption that $\Delta\phi$ has no wavelength-dependence. For a wavelength-dependent phase shift, $\Delta\phi(\lambda)$, which has a π phase shift for the central wavelength, λ_0, we have:

$$\Delta\phi(\lambda_0) = \pi = \frac{2\pi}{\lambda_0}\Delta nL \tag{B.12}$$

where Δn is the change of waveguide refractive index required for the π phase shift for λ_0; L is waveguide length. Accordingly, $\Delta\phi(\lambda)$ can be given by:

$$\Delta\phi(\lambda) = \frac{2\pi}{\lambda}\Delta nL = \frac{\lambda_0}{\lambda}\pi \tag{B.13}$$

where λ is operation wavelength. By substituting Eq. B.13 into Eqs. B.4 and B.5, wavelength-dependent performance at the bar state can be calculated. As $\frac{\lambda_0}{\lambda}$ is close to 1 (considering a 100 nm wavelength span centred at 1550 nm), we obtain:

$$P_{out1}(\lambda) \approx (\kappa^2+t^2)^2 \tag{B.14}$$

$$P_{out2}(\lambda) \approx 0 \tag{B.15}$$

$$ER_{bar}(\lambda) = 10\log_{10}(\frac{P_{out1}(\lambda)}{P_{out2}(\lambda)}) \approx \infty \tag{B.16}$$

which indicates that the wavelength-dependent bar state ER is insensitive to κ^2 and t^2.

Appendix C

Derivation of Coupling Ratios Extractions for 2×2 Couplers

As per Appendix B, the responses of a MZI circuit are sensitive to the coupling ratios, κ^2 and t^2, of its 2×2 couplers. Conversely, the responses of a MZI circuit can be used to characterize the κ^2 and t^2 of 2×2 couplers.

For a MZI circuit with imbalanced phase arms, as illustrated in Fig. B.1, each output transmission will go through minima and maxima when sweeping the operation wavelength, due to the wavelength-dependent phase delay, $\Delta\phi(\lambda)$. Based on the output transmission functions given by Eqs. B.4 and B.5, we define interference extinction ratio (IER) for each output port, which is the difference on a logarithmic scale between minima and maxima transmissions, as given by:

$$IER_{out1} = 10\log_{10}\left(\frac{P_{out1,max}}{P_{out1,min}}\right) = 10\log_{10}\left(\frac{(\kappa^2+t^2)^2}{(\kappa^2-t^2)^2}\right) \tag{C.1}$$

$$IER_{out2} = 10\log_{10}\left(\frac{P_{out2,max}}{P_{out2,min}}\right) = 10\log_{10}\left(\frac{4\kappa^2 t^2}{0}\right) = \infty \tag{C.2}$$

where $P_{out1,max}$ and $P_{out1,min}$ are maxima and minima transmissions at the output 1, respectively; $P_{out2,max}$ and $P_{out2,min}$ maxima and minima transmissions at the output 2, respectively. According to the results, IER$_{out1}$ is dependent to κ^2 and t^2, and therefore the spectral responses at output 1 can be used to characterize κ^2 and t^2; however, IER$_{out2}$ is independent to κ^2 and t^2, and hence the spectral responses at output 2 is invalid for characterization.

Assuming the 2×2 couplers are lossless, i.e., $\kappa^2 + t^2 = 1$, based on Eq. C.1, the extracted coupling ratios are given by:

$$\kappa^2 = \frac{1}{2}(1 \pm \frac{1}{\sqrt{10^{\frac{IER_{out1}}{10}}}}) \tag{C.3}$$

$$t^2 = 1 - \kappa^2 \tag{C.4}$$